

Solvation of Mg in Helium-4: Are there Meta-stable Mg Dimers?

Eckhard Krotscheck^{1,2a}, Robert E. Zillich^{2b}

¹*Department of Physics, University at Buffalo SUNY, Buffalo NY 14260, USA*

²*Institute for Theoretical Physics, Johannes Kepler Universität Linz,
Altenbergerstraße 69, A-4040 Linz, Austria*

(Dated: March 9, 2022)

Abstract

Experiments on the formation of magnesium complexes in ^4He nanodroplets were interpreted as the observation of the formation of weakly bound magnesium complexes. We present results for single Mg and Mg dimer solvation using the hypernetted chain / Euler-Lagrange method as well as path integral Monte Carlo simulations. We find that the phonon-mediated, indirect Mg-Mg interaction adds an oscillatory component to the direct Mg-Mg interaction. We undertake a step-by-step examination of the ingredients of the calculation of the phonon-induced interaction, comparing the results of semi-analytic HNC-EL calculations for bulk and single impurity results with experiments as well as Monte Carlo data. We do not find evidence for a sufficiently strong secondary minimum in the effective Mg-Mg interaction to support a metastable state.

^a Electronic address: eckhardk@buffalo.edu

^b Electronic address: robert.zillich@jku.at

I. INTRODUCTION

Experiments by Przystawik *et al.*¹ on the formation of magnesium complexes in ^4He nanodroplets were interpreted as the observation of the formation of weakly bound magnesium complexes, dubbed “bubble foam”, which collapsed to form dense Mg clusters upon laser excitation. In the same work, as well as in Ref. 2, calculations based on a density functional theory (DFT) for helium found that the effective interaction potential between two Mg atoms has a local minimum at a separation of about 10\AA and 2-3 K deep. The presence of such a minimum would support the interpretation that indeed a weakly bound “bubble foam” can form in helium where Mg atoms are separated from each other by a layer of ^4He atoms. The mean lifetime of a metastable dimer state was, however, estimated to be many orders of magnitude too short to explain the experiment. Such a predicted dimer could only in a highly excited rotational state be stable on the time scale of the experiment.

We examine in this work the effective interaction potential between two Mg atoms solvated in ^4He using both a semi-analytic approach based on optimized pair and triplet correlations quantum Monte Carlo simulations. We expect that, if weakly bound Mg dimers can form, this would be a local effect and not be affected by the presence of the droplet surface. That means that such an effect would be observable in small and large ^4He droplets as well as in bulk ^4He . To determine if such a bound state can exist, we perform calculations of Mg impurities in bulk ^4He using the hypernetted chain / Euler-Lagrange (HNC-EL) method. HNC-EL yields the effective potential $V_{\text{eff}}(r)$ felt by two Mg atoms inside helium which consist of the bare interaction and an oscillatory induced potential mediated by phonons in the surrounding He. We show that these oscillations are not strong enough to lead to pronounced secondary minima of $V_{\text{eff}}(r)$. We have carefully examined hydrodynamic consistency of all ingredients, and the importance of so-called elementary diagrams and triplet correlations and find these negligible at distances where a metastable state would exist.

As far as computationally efficient, we compare our HNC-EL results for single Mg in bulk helium with corresponding path integral Monte Carlo (PIMC) simulations where we found excellent agreement. Furthermore we have performed simulations of Mg dimers and trimers in small droplets of up to 100 ^4He atoms. Again, we did not observe the formation of weakly bound Mg complexes but instead observed a swift equilibration to the ground state.

II. METHODOLOGY

In this work we employ two complementary methods, a semi-analytic approach using diagrammatic quantum many-body theory, and a computational approach using quantum Monte Carlo simulation. Both methods employ the full many-body Hamiltonian of N ^4He atoms (indexed by Latin subscripts) and one or more Mg impurities (indexed by Greek subscripts)

$$H = -\frac{\hbar^2}{2M} \sum_{\alpha} \nabla_{\alpha}^2 - \frac{\hbar^2}{2m} \sum_{i=1}^N \nabla_i^2 + \sum_{\alpha,i} V_{AHe}(|\mathbf{r}_{\alpha} - \mathbf{r}_i|) + \sum_{i<j} V_{HeHe}(|\mathbf{r}_i - \mathbf{r}_j|) \quad (1)$$

where m and M are the masses of a ^4He and Mg atom, respectively. In this Hamiltonian we assume pair-wise interactions which is known to be a reliable approximation for atoms in their electronic ground state. We assume that the ^4He atoms interact via the Aziz-II potential³. This potential reproduces the equation of state of ^4He with high accuracy⁴. For the interaction $V_{AHe}(\mathbf{r}_{\alpha} - \mathbf{r}_i)$ between the host liquid and the impurity atom we have used the potential models by Hinde⁵ *et al.* and, for comparison, the one by Partridge *et al.*⁶. For the Mg-Mg interaction we have used the potential by Tiesinga *et al.*⁷.

A. Hypernetted-chain Euler-Lagrange

1. ^4He background calculation

The Hypernetted chain/Euler-Lagrange method is a well established fast and accurate method for calculating properties of strongly interacting quantum fluids. The method has been described in numerous review articles and pedagogical material, see, for example, Ref. 8. The wave function is expanded in a Jastrow-Feenberg form in terms of multiparticle correlation functions $u_n(\mathbf{r}_1, \dots, \mathbf{r}_n)$, truncation at $n = 3$ is normally sufficient.

$$\Psi_0(\mathbf{r}_1, \dots, \mathbf{r}_N) = \exp \frac{1}{2} \left[\sum_{i<j} u_2(\mathbf{r}_i, \mathbf{r}_j) + \sum_{i<j<k} u_3(\mathbf{r}_i, \mathbf{r}_j, \mathbf{r}_k) + \dots \right]. \quad (2)$$

The correlation functions $u_n(\mathbf{r}_1, \dots, \mathbf{r}_n)$ are determined by minimization of the energy-expectation value E_0

$$\frac{\delta E_0}{\delta u_n(\mathbf{r}, \dots, \mathbf{r}_n)} = 0. \quad (3)$$

The energy expectation value and other physically relevant quantities are calculated by diagrammatic expansions. The hierarchy of “hypernetted chain” integral equations provides a scheme that is, at every level of implementation, consistent with the optimization problem (3) in the sense that the resulting pair distribution and structure functions reproduce *qualitatively* the properties of the solution of the exact variational problem.

For the problem at hand, we only need the static structure function $S(k)$ for bulk helium. For long wavelengths, the static structure function goes as

$$S(q) = \frac{\hbar q}{2mc} \quad \text{as } q \rightarrow 0 \quad (4)$$

where c is the speed of sound obtained from a theory of excitations or from the equation of state

$$mc^2 = \frac{d}{d\rho} \rho^2 \frac{d(E/N)}{d\rho}. \quad (5)$$

The c obtained from the equation of state will normally be *different* from the speed of sound obtained from the slope of $S(q)$, in fact these two quantities agree only in an exact theory. However, the inconsistency is weak and can be repaired by a slight phenomenological modification of the Euler equation for the triplet correlation function which has no visible consequences on the equation of state⁹.

2. Single impurity calculation

In the next step, the impurity is included. The wave function of the compound system is

$$\Psi^I(\mathbf{r}_0, \mathbf{r}_1, \dots, \mathbf{r}_N) = \exp \frac{1}{2} \left[\sum_{j=1}^N u^I(\mathbf{r}_0, \mathbf{r}_j) + \frac{1}{2!} \sum_{\substack{j,k=1 \\ j \neq k}}^N u^I(\mathbf{r}_0, \mathbf{r}_j, \mathbf{r}_k) \right] \Psi(\mathbf{r}_1, \dots, \mathbf{r}_N). \quad (6)$$

The *chemical potential* of the impurity is the energy gained or lost by adding one impurity particle into the liquid, in other words it equals to the energy difference

$$\begin{aligned} \mu^I &= E_{N+1} - E_N \\ &= \frac{\langle \Psi^I | H^I | \Psi^I \rangle}{\langle \Psi^I | \Psi^I \rangle} - \frac{\langle \Psi | H | \Psi \rangle}{\langle \Psi | \Psi \rangle}. \end{aligned} \quad (7)$$

and the Euler equation are derived by minimizing the impurity chemical potential. Results are again the energetics as well as structure and distribution functions.

There is again a hydrodynamic consistency condition between the long wavelength limit of the static structure function and the density dependence of the chemical potential: The long wavelength limit of the impurity–background (“IB”) structure function is¹⁰

$$S_{IB}(q) = -\alpha \quad \text{as } q \rightarrow 0 \quad (8)$$

where α is the volume excess factor

$$\alpha = \frac{\rho}{mc^2} \frac{d\mu_I}{d\rho}. \quad (9)$$

The volume excess factor α can be calculated from $S_{IB}(0+)$ and from the density dependence of the impurity binding energy. Again, the long wavelength limit (8) and the hydrodynamic derivative (9) agree only in an exact theory. By the same slight phenomenological modification of the three-body correlation function that enforces the consistency between the speed of sound obtained by Eqs. (4) and (5) and does not affect the impurity binding energy visibly, the two quantities can be made consistent.

3. Impurity-impurity interaction

In the case of two impurities, located at \mathbf{r}_0 and \mathbf{r}'_0 , the wave function is

$$\begin{aligned} \Psi^{II}(\mathbf{r}_0, \mathbf{r}'_0; \mathbf{r}_1, \dots, \mathbf{r}_N) = & \exp \frac{1}{2} \left[u^{II}(\mathbf{r}_0, \mathbf{r}'_0) + \sum_{j=1}^N [u^{IB}(\mathbf{r}_0, \mathbf{r}_j) + u^{IB}(\mathbf{r}'_0, \mathbf{r}_j) + u^{IIB}(\mathbf{r}_0, \mathbf{r}'_0, \mathbf{r}_j)] \right. \\ & \left. + \frac{1}{2!} \sum_{\substack{j,k=1 \\ j \neq k}}^N [u^{IBB}(\mathbf{r}_0, \mathbf{r}_j, \mathbf{r}_k) + u^{IBB}(\mathbf{r}'_0, \mathbf{r}_j, \mathbf{r}_k)] \right] \Psi_0(\mathbf{r}_1, \dots, \mathbf{r}_N). \quad (10) \end{aligned}$$

The situation for the two impurity case differs from the above ones because the wave function (10) can only lead to an effective impurity-impurity potential determining the impurity–impurity correlation function $u^{II}(\mathbf{r}_0, \mathbf{r}'_0)$. This is exactly the quantity we want because it gives us the information on the configuration. Its form has, in HNC approximation, been first derived by Owen¹¹; adding “elementary diagram” and “triplet correlation” corrections, the effective interaction is

$$V_{eff}(r) = V^{(II)}(r) + V_e(r) + w_{\text{ind}}(r) \quad (11)$$

where $V^{(II)}(r)$ is the bare interaction between the two impurities, $V_e(r)$ the correction from “elementary” diagrams and triplets, and $w_{\text{ind}}(r)$ is the induced interaction originating from

phonon exchange and higher-order processes. The induced potential can depend only on background and single-impurity quantities. The “elementary diagram” correction is calculated within the usual diagrammatic expansion methods¹². The induced potential from triplet calculations is new; it is best calculated taking the two-impurity limit of the mixture theory¹³. Since triplet correlations turn out to cause a negligible correction we refrain from giving the somewhat tedious derivation.

Jastrow-Feenberg theory provides a prescription for calculating the induced Mg-Mg potential mediated by the density fluctuations in the He liquid, *i.e.* phonon exchange¹¹

$$\tilde{w}_{\text{ind}}(k) = \tilde{V}_{\text{ind}}(k, \bar{\omega}(k)) = -\frac{\hbar^2 k^2}{4m} \left[\frac{S_{IB}(k)}{S(k)} \right]^2 \left[2\frac{m}{m_I} S(k) + 1 \right]. \quad (12)$$

One can interpret this term from linear response theory: The full interaction between two Mg atoms is strictly speaking energy dependent, it is the sum of the induced and the bare interaction,

$$V_{\text{eff}}(r, \omega) = V_{\text{Mg-Mg}}(r) + V_{\text{ind}}(r, \omega) \quad (13)$$

where

$$\tilde{V}_{\text{ind}}(k, \omega) = \tilde{V}_{IB}(k) \chi(k, \omega) \tilde{V}_{IB}(k) + \tilde{V}_e(k) \quad (14)$$

and $\chi(k, \omega)$ is the density-density response function of bulk helium, V_{ph}^{IB} is the particle-hole potential, and $\tilde{V}_e(k)$ consists of contributions from triplets and elementary diagrams. The HNC-EL result is obtained by taking the density-density response function at an *average* imaginary frequency¹⁴ that is chosen according to the localization rules of parquet-diagram theory^{15–18}.

If one looks at the phonon exchange of weakly bound pairs of Mg atoms, one might therefore argue that it is better to take $\omega = 0$ which leads to a slightly different effective interaction

$$\tilde{w}'_{\text{ind}}(k) = \tilde{V}_{\text{ind}}(k, \omega = 0) = -\frac{\hbar^2 k^2}{4m} \left[\frac{S_{IB}(k)}{S(k)} \right]^2 \left[\frac{m}{m_I} S(k) + 1 \right]. \quad (15)$$

We will see, however, that there is little difference between the predictions of these two procedures for calculating the induced interaction.

B. Path integral Monte Carlo

Path integral Monte Carlo (PIMC) exploits the isomorphism between quantum theory and a classical system of closed polymer chains^{19,20}. For bosons, like ⁴He atoms, PIMC is

an exact finite-temperature method. In PIMC the configuration space representation of the many-body density matrix $\rho(\mathbf{r}, \mathbf{r}'; \beta) = \langle \mathbf{r} | e^{-\beta \hat{H}} | \mathbf{r}' \rangle$, where $\beta = 1/k_B T$, is sampled by the Metropolis algorithm²¹. For the evaluation of $\rho(\mathbf{r}, \mathbf{r}'; \beta)$, the “imaginary time” interval β is split into smaller time steps $\tau = \beta/M$ which necessitates the introduction of new coordinates at intermediate time slices,

$$\rho(\mathbf{r}_0, \mathbf{r}_M; \beta) = \int d\mathbf{r}_1 \cdots \mathbf{r}_{M-1} \rho(\mathbf{r}_0, \mathbf{r}_1; \tau) \cdots \rho(\mathbf{r}_{M-1}, \mathbf{r}_M; \tau). \quad (16)$$

In the above equation, $(\mathbf{r}_0, \dots, \mathbf{r}_M)$ is a discretized path in imaginary time. For sufficiently small τ , $\rho(\mathbf{r}_0, \mathbf{r}_1; \tau)$ can be approximated in various ways; here we use the pair density approximation²². If only averages of diagonal operators are required (such as energy or density distributions), we set $\mathbf{r}_M = \mathbf{r}_0$. Finally, Bose symmetry is implemented by symmetrization of the density matrix

$$\rho_B(\mathbf{r}, \mathbf{r}; \beta) = \frac{1}{N!} \sum_P \rho(\mathbf{r}, P\mathbf{r}; \beta) \quad (17)$$

which corresponds to reconnecting the imaginary time paths to form larger chains. For a detailed review of the PIMC method for bosons see Ref. 22, for the application to dopants in ⁴He clusters see Ref. 23,24. Bulk simulations are implemented by invoking periodic boundary conditions. We put 256 ⁴He atoms together with the Mg atom in a cubic simulation box of the side length L which is determined by the condition that the pair density $\rho_{IB}(r)/\rho_I$ approaches the equilibrium density of bulk ⁴He, $\rho = 0.02186 \text{ \AA}^{-3}$, for large distance r . Due to the periodic boundary conditions, the maximal distance is typically $L/2 \approx 11 \text{ \AA}$, which is not large enough that $\rho_{IB}(r)/\rho_I$ can be considered constant. Therefore the choice of L is somewhat ambiguous. This leads to some uncertainty in the energy calculation to be discussed below.

III. RESULTS

A. A single Mg impurity in bulk ⁴He

1. Energetics.

Fig. 1 shows HNC-EL results for the chemical potential of a single Mg atom as a function of density, calculated for our two potential models. Also shown is the volume excess factor α .

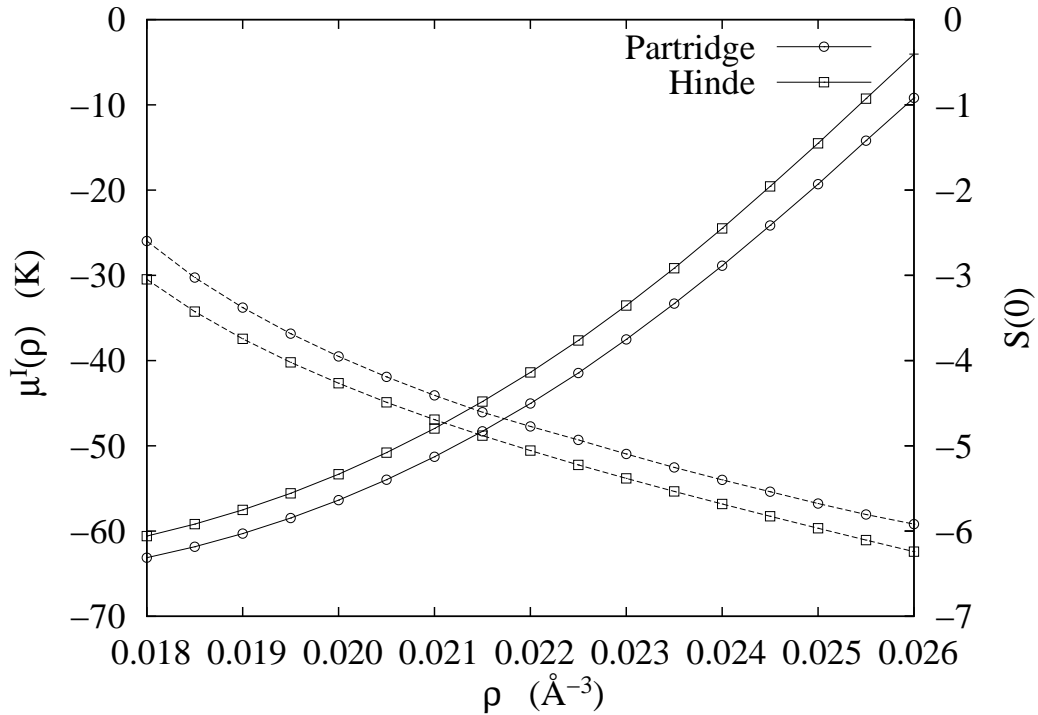


FIG. 1: The figure shows the chemical potential of a single Mg impurity in liquid ${}^4\text{He}$ as a function of density for the Partridge⁶ (circles) and the Hinde⁵ potentials (boxes) (solid lines, left scale). We also show the volume coefficient $-\alpha = S(0+)$ for the same two potentials (dashed lines, right scale).

Monte Carlo calculations of the Mg chemical potential in bulk ${}^4\text{He}$ are computationally very expensive because the chemical potential is a quantity of order $O(N^0)$ and has to be extracted from the differences of total energies which are of order $O(N^1)$. Due to the large size of the Mg atom, correlated sampling as used *e.g.* in Ref. 25 for an ${}^3\text{He}$ impurity is not possible here. HNC-EL calculations are, compared to this, many orders of magnitude faster. Their accuracy also suffers from the large core of the He-Mg interaction which has the consequence that “elementary diagrams”, which contribute only a relatively small amount to the binding energy of ${}^4\text{He}$, are a large effect in the problem at hand. We note, however, that the binding energy of a single Mg impurity is only of secondary interest for our purpose; the more relevant quantity is the static structure function $S_{IB}(k)$ and in particular the consistency of $S_{IB}(0+)$ with the volume coefficient α , *cf.* Eq. (8). We have therefore focused our attention to computing the static structure function $S_{IB}(k)$ with PIMC which is not plagued by the difficulty of being the difference of two big numbers.

2. Structure.

The most interesting quantities are the static structure function and the pair distribution function. DMC and PIMC calculations for the Mg-He distribution function $g_{IB}(r)$ and the static structure function $S_{IB}(k)$ are much less demanding than energy calculations. A similar statement applies for the HNC calculations: The largest uncertainty in the calculation is how “elementary diagrams” are dealt with. While these diagrams have a rather visible effect on the energetics, they produce only a modest enhancement of the nearest neighbor peak in the pair distribution function and a practically invisible correction to the static structure function.

Figs. 2 and Figs. 3 show the HNC-EL and PIMC results for the pair distribution function and the static structure function. We find very good agreement between these results within statistical uncertainties, confirming that both methods provide the same high level of accuracy. As expected, the simulation results gave somewhat larger uncertainties at long wave lengths, but the comparison with HNC-EL calculations and the hydrodynamic consistency condition are encouraging. Fig. 3 also show the $S_{IB}(k)$ that is obtained without enforcing hydrodynamic consistency. Evidently the difference is small, but it appears that the consistent $S_{IB}(k)$ agrees somewhat better with Monte Carlo calculations.

B. Single Mg impurity in ^4He clusters

The Mg-He interaction is quite weak, it has therefore been suggested that Mg is not solvated inside a He cluster but might be the cluster surface. In a careful study using diffusion Monte Carlo, Mella *et al.*²⁶ indeed showed that the energetic balance for Mg is very delicate, and the solvation structure indeed depends on the details of the Mg-He interaction. For the potential used in this work⁵, Mella *et al.* predicted that the Mg resides inside $^4\text{He}_N$ clusters at $T = 0$, if N is larger than $N_{\text{crit}} \approx 25$. DFT calculations gave similar results².

We have performed PIMC simulations of a single Mg impurity in ^4He clusters mainly to confirm or refute this prediction for $T > 0$. We have chosen $T = 0.31\text{K}$ and $T = 0.62\text{K}$, while He droplets produced in experiment have an estimated temperature of about $T = 0.3 - 0.4\text{K}$. In the left panel of Fig. 4 we show the Mg density $\rho_I(r)$ with respect to the center of mass of the $^4\text{He}_N$ cluster. The probability density for Mg situated at distance r from the center mass

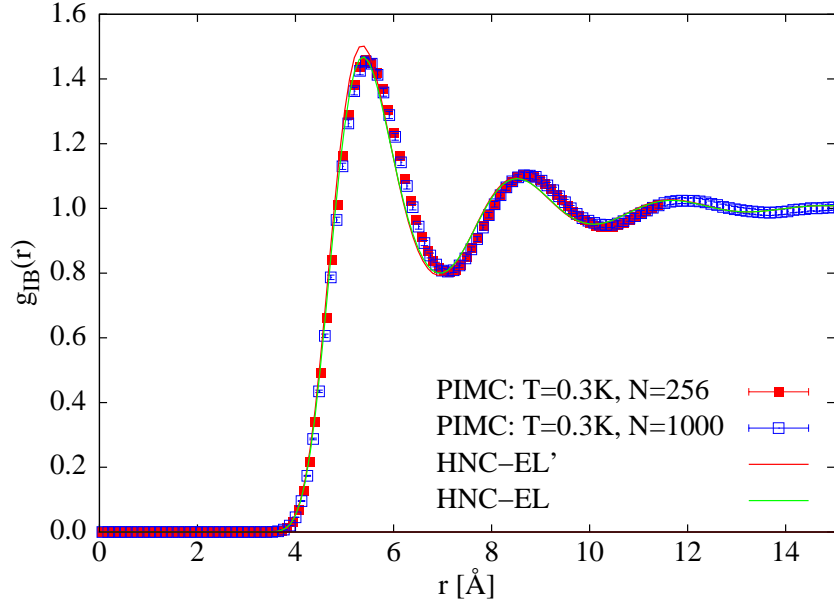


FIG. 2: Comparison of the pair distribution function between Mg and ${}^4\text{He}$ in bulk helium, $g_{IB}(r)$, between HNC-EL and PIMC. The HNC-EL calculation was done with and without enforcing hydrodynamic consistency. The PIMC simulations were done at $T = 0.31\text{K}$ for two system sizes, $N = 256$ and $N = 1000$.

is given by $4\pi r^2 \rho_I(r)$ and is shown in the right panel. We chose $N = 100$ to be safely in the regime where Mg is predicted to be inside the He cluster at $T = 0$. Indeed, at the lower end of the temperature estimated in experiments, at $T = 0.31\text{K}$, the most probable location of Mg is in the center of the He cluster. The situation changes drastically, as the temperature is raised to $T = 0.62\text{K}$, slightly above the experimental estimate. The Mg density $\rho_I(r)$ now has a shoulder at large distance for the He cluster center. The right panel showing $4\pi r^2 \rho_I(r)$ shows that the most probable location of Mg is now at the surface of ${}^4\text{He}_{100}$. This strong dependence of the Mg location on the temperature around the experimental He droplet temperature indicates that slight disturbances of the He cluster may cause large movements of the Mg impurity.

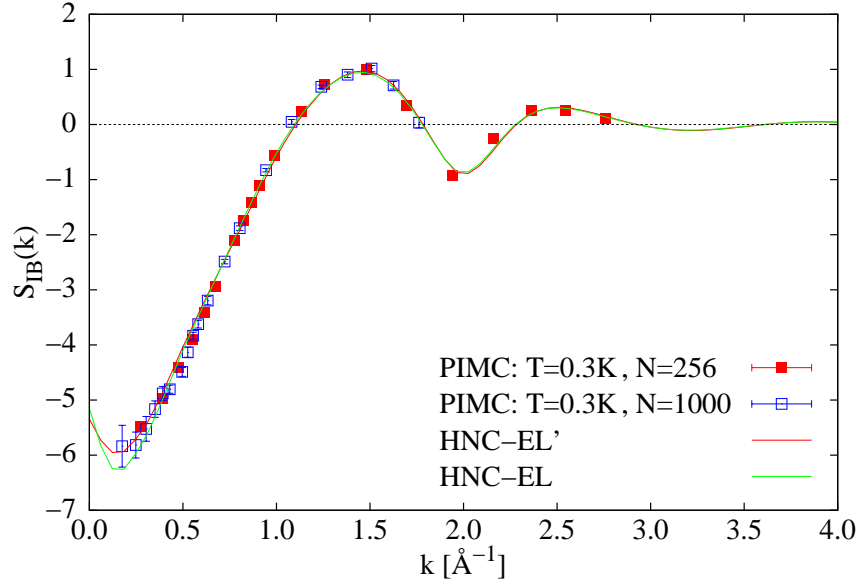


FIG. 3: Same as Fig. 2 for the static structure function $S_{IB}(k)$.

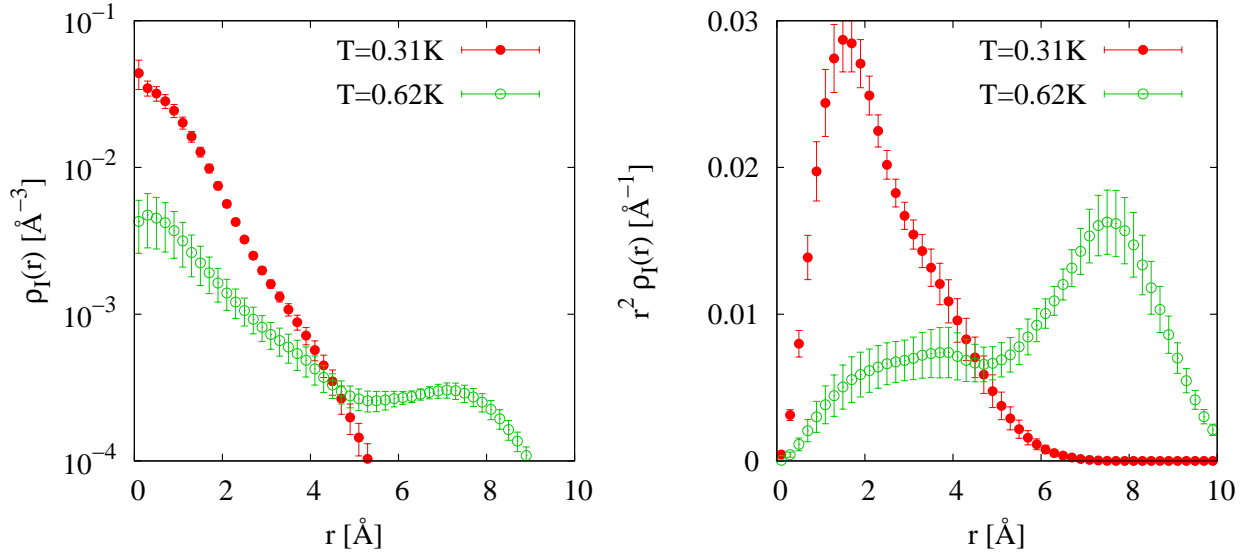


FIG. 4: Left: Mg density $\rho_I(r)$ with respect to the center of mass of the ${}^4\text{He}_N$ cluster, $N = 100$, at $T = 0.31\text{K}$ and $T = 0.62\text{K}$. Right: corresponding plot $r^2\rho_I(r)$. The Mg impurity is clearly located inside the He cluster for $T = 0.31\text{K}$, while for $T = 0.62\text{K}$ it is more likely to reside on the surface.

C. HNC-EL for the dimer interaction

The key result of our calculations is the effective interaction (11). Figs. 5 and 6 show the HNC-EL results for the effective interaction, using the two versions (12) and (15) of the

induced interaction defined above. Hydrodynamic consistency was enforced as described in section II A. The figures also give information on the importance of elementary diagram corrections and triplet correlations. It is seen that the effect of triplet correlations is almost invisible; elementary diagrams modify the effective interaction only at short distances and can, therefore, have a visible influence on the binding energy of the Mg dimer in its ground state.

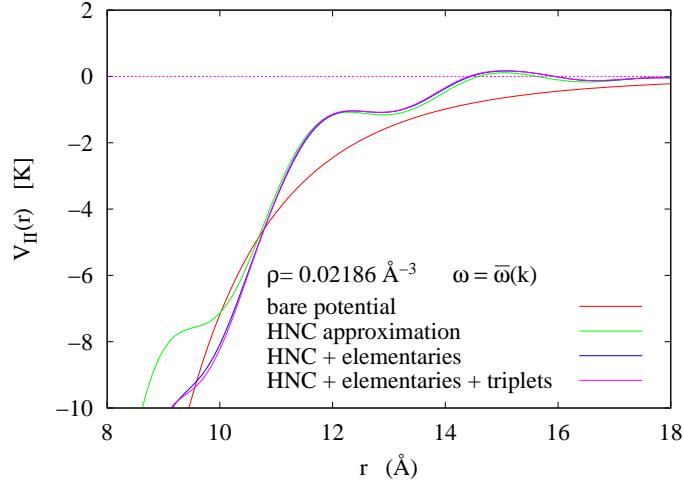


FIG. 5: Effective Mg-Mg potential $V_{\text{eff}}(r)$, consisting of the bare Mg-Mg interaction (full) and the induced interaction $w_{\text{ind}}(r)$ given by Eq. (12). The three dashed lines show $V_{\text{eff}}(r) + w_{\text{ind}}(r)$ for the three increasingly accurate approximations: HNC-EL without elementary diagrams and triplet correlations; inclusion of elementary diagrams; inclusion of both elementary diagrams and triplet correlations.

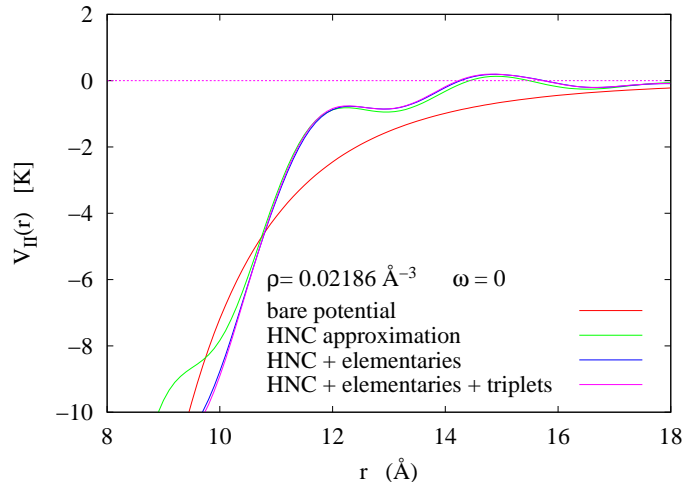


FIG. 6: As Fig. 5, but choosing an average frequency $\bar{\omega} = 0$, Eq. (15).

The results of both versions of the induced interaction are practically identical, the version using the zero-frequency response function is only slightly more repulsive. We see in both cases two slight local maxima at distances of about 12 \AA and 14.4 \AA . However these maxima are much too weak to permit a metastable loosely bound state at large distances. We have also calculated the bound state energies of the Mg dimer; there is no evidence for an increased density of states in the energy regime where the effective potential becomes oscillatory.

D. PIMC simulation of Mg dimers

We have also performed PIMC simulations for a Mg dimer surrounded by a cluster of either 100 or 200 ^4He atoms at a temperature of $T = 0.31\text{K}$, which is on the low end of the estimated temperature of ^4He droplets, $T = 0.3 - 0.4\text{K}$, in typical experimental conditions²⁷. Already such a small ^4He droplet might be able to form a “protective” ^4He layer between two Mg atoms, respectively, that was invoked in Ref. 28 to explain why weakly bound Mg complexes can be stable against collapse to the ground state.

Our search for a metastable Mg dimer state consists of three stages to make the equilibration of the Mg degrees of freedom as gentle as possible: (i) equilibrating ^4He atoms with the two Mg atoms held fixed at a distance of 10 \AA (ii) releasing the Mg atoms to allow them to equilibrate, but *without* the bare Mg-Mg interaction – hence only the effective phonon-mediated interaction $V_{\text{ind}}(r)$ is felt by the Mg. Our HNC-EL calculation has shown that $V_{\text{ind}}(r)$ is oscillating with r and thus has local minima; (iii) switching on the bare Mg-Mg interaction.

In stage (ii), the two Mg atoms indeed stay well separated by approximately 10 \AA . Hence the local minima of just the phonon-mediated effective interaction $V_{\text{ind}}(r)$ indeed support bound states of a well-separated Mg pair. Note that this is a metastable state since the ground state would correspond to the Mg atoms coalescing to the same spot since there is no bare Mg-Mg interaction preventing this. Fig. 7 shows the ^4He density with respect to the Mg-Mg axis for $N = 100$ and $N = 200$.

The ^4He density is not zero between the two Mg atoms in the dimer; these are separated by a liquid layer of helium. Note that this result also demonstrates that PIMC simulations can sample a metastable state, where we take advantage that PIMC does not necessarily ergodically sample the full configuration space in the presence of a high reaction barrier.

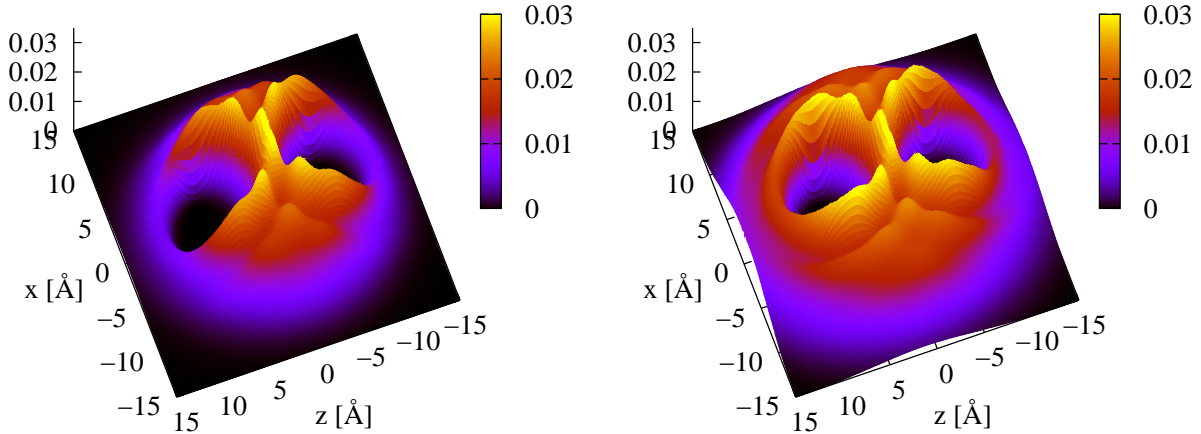


FIG. 7: ${}^4\text{He}$ density $\rho(\mathbf{r})$ in the coordinate frame defined by the instantaneous Mg-Mg axis for a cluster of $N = 100$ (left) and $N = 200$ (right) ${}^4\text{He}$ atoms.

For example, we have observed such a metastable state for electronically excited Rb on the surface of helium by performing a “vertical Monte Carlo” transition from the $\Sigma_{1/2}$ to the $\Pi_{1/2}$ and $\Pi_{3/2}$ states^{29,30}, in agreement with experiment³¹.

However, these simulations obtained by non-ergodic sampling do not yet provide information on the height of barrier for the two Mg atoms to coalesce to the same spot, *i.e.* whether the He layer between two Mg atoms prevents the formation of Mg_2 in its ground state when the bare Mg-Mg interaction is turned on. To calculate the energy that the Mg dimer has to overcome, we performed simulations as in stage (i), but fixing the Mg atoms at varying distance r and recorded the total energy E as function of r . This corresponds to a Born-Oppenheimer approximation for the He surrounding the Mg atoms, where the Mg atoms are effectively assumed to have infinite mass. In HNC-EL, the proper bare mass of Mg is used. A comparison between $\tilde{w}_{\text{ind}}(k)$, Eq. (12), in Fig.5 and $\tilde{w}'_{\text{ind}}(k)$, Eq. (15), in Fig. 6 shows that, at least for the HNC-EL induced interaction, the mass of Mg has only a small influence.

The energy $E(r)$ is shown in Fig. 8, together with the induced Mg-Mg potential calculated by HNC-EL according to Eq. (12). The agreement between the HNC-EL results and the PIMC calculations is excellent if hydrodynamic consistency is ensured (see section IIA, considering that very different approximations are made for the HNC-EL calculations (variational wave function, approximation for elementary diagrams) and PIMC calculations (Born-Oppenheimer approximation), respectively).

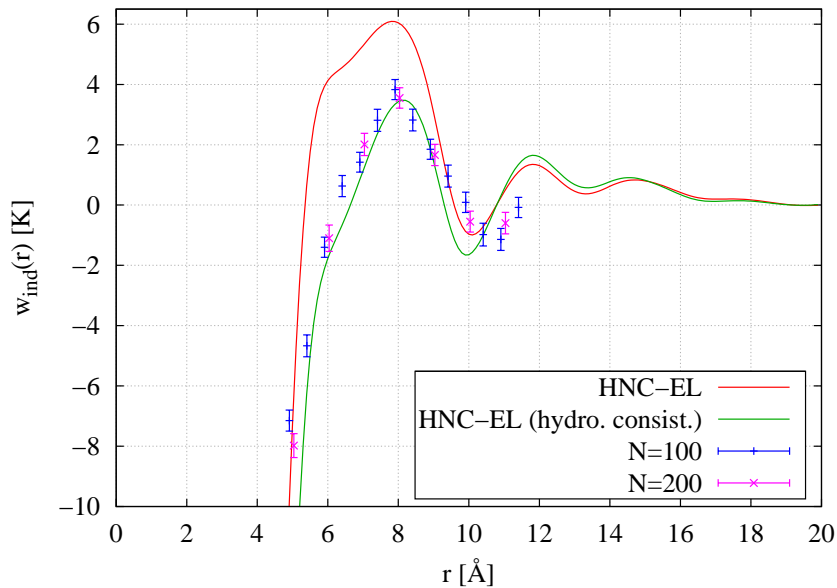


FIG. 8: Comparison of the *induced* Mg-Mg potential between HNC-EL for bulk ${}^4\text{He}$ (red/green: without/with hydrodynamic consistency) and PIMC at $T = 0.31\text{K}$, for clusters of $N = 100$ (blue) and $N = 200$ (pink) ${}^4\text{He}$ atoms. The latter curve was obtained by subtracting X K and Y K from the total energy obtained by PIMC.

In Fig. 9, we add the bare Mg-Mg interaction to $V_{\text{ind}}(r)$ to obtain the full interaction $V_{\text{eff}}(r)$ felt by a pair of Mg atoms. The tenuous local minimum of the He-induced interaction clearly has a barrier much too small to survive when the bare Mg-Mg interaction is added.

In stage (*iii*) in our PIMC investigation, we finally turn on the bare Mg-Mg interaction. From the above calculation of the $V_{\text{eff}}(r)$ in Born-Oppenheimer approximation we expect that the Mg pair will equilibrate from the weakly-bound metastable state observed without the bare Mg-Mg interaction in stage (*ii*) to a strongly bound state. This is indeed what happens in every PIMC simulation, trying 16 different initial configurations obtained in stage (*ii*). We did not find evidence for a weakly bound dimer state, when all interaction of the Hamiltonian are included in the simulations. Instead we always observe swift equilibration to the dimer ground state. While this PIMC result itself does not constitute a proof that there is no weakly bound metastable dimer, the Born-Oppenheimer potential energy together with the HNC-EL results make a compelling case that such a state is highly unlikely.

We also investigated the (meta-)stability of Mg trimers. Starting with three Mg atoms situated at large distance from each other in a triangle, PIMC simulations without the bare

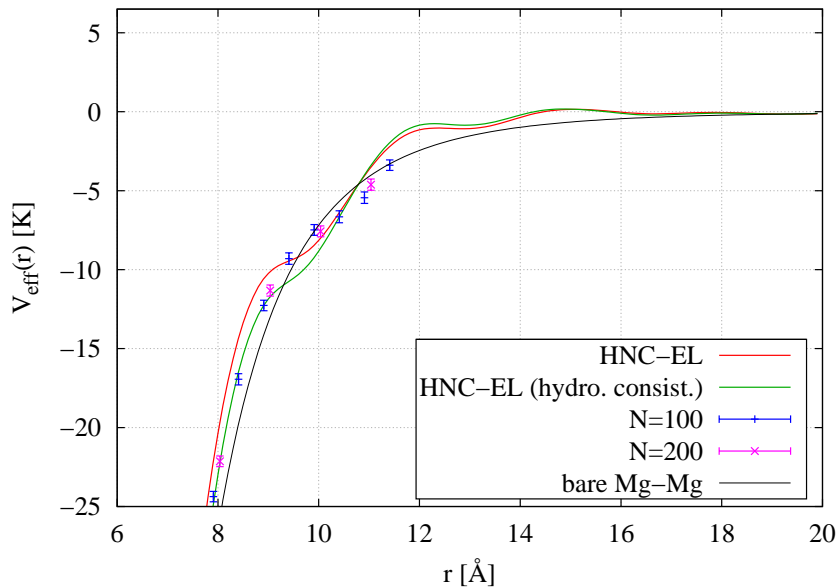


FIG. 9: Same as Fig. 8, but for the effective Mg-Mg potential $V_{\text{eff}}(r)$, i.e. adding the bare interaction according to Eq. (13).

Mg-Mg interactions equilibrated towards metastable states similar to the corresponding simulations of Mg dimers, *i. e.* each Mg solvated by a protective layer of He instead of the three Mg collapsing to the same spot. However, as for Mg dimers, turning on the bare Mg-Mg interactions quickly lead to Mg_3 equilibrating towards the trimer ground state.

IV. CONCLUSION

The main goal of our work was to investigate the effective potential barrier with two alternative and manifestly microscopic theoretical methods. We have used the variational HNC-EL method, based on Jastrow-Feenberg wave functions which include correlations between He atoms and between He and the molecule, which are absent in DFT. Due to the increased complexity due to correlations we have restricted ourselves to Mg atoms in bulk ^4He . Additionally, we used PIMC to simulate Mg atoms in bulk ^4He and in small droplets of ^4He . We found very good agreement of the solvation structure around an Mg atoms, described by the static structure function. We also confirmed that Mg atoms reside inside He sufficiently large droplets, but only barely – slightly elevating the temperature leads to significant population of surface states.

We have also derived approximate Mg-Mg-He triplet correlations based on the HNC-EL results for a single impurity, and from that the induced Mg-Mg interaction, *i.e.* the effective interaction mediated by excitation of the surrounding He medium. Since PIMC simulations of two widely separated Mg atoms in bulk He would be computationally very demanding, we opted for two Mg atoms in small ^4He clusters, of $N = 100$ and 200 atoms. Furthermore, simulations where the two Mg atoms can move freely among the He atoms very quickly find the stable ground state of a closely bound Mg dimer, despite starting the simulations with a large initial separation between the Mg atoms. Therefore, we had to use a Born-Oppenheimer approximation, where the heavier Mg atoms are held fixed at distance R while the He atoms are allowed to move in the simulation. Repeating the simulation for many different R maps out the effective interaction between the Mg atoms. Since Mg atoms are only six times heavier than He atoms, we should expect an effective interaction biased by the Born-Oppenheimer approximation; we note that the DFT estimates of Ref. 2 also used this Born-Oppenheimer approximation.

The most severe potential inaccuracy of the Born-Oppenheimer approximation is, however not because of the mass of the Mg atoms as discussed above, but due to the dynamic coupling of the zero-point motion of the dimer to the surrounding helium through hydrodynamic backflow. In fact, one would expect that this backflow effect is different dependent on whether the dimer is in an excited state or in the ground state. A quantitative assessment of the effect is very difficult and the theoretical tools are presently not available. We have therefore estimated the effective mass using the methods of Ref.³² and found a value of $m^*/m \approx 2$. This mass enhancement is still far from what would be needed to generate a sufficiently long-lived metastable state in the relative potential minimum around 10 \AA .

We found that neither the HNC-EL results nor the PIMC results for the induced Mg-Mg interaction supports a local minimum in the total effective interaction consisting of bare and induced interaction. The results for the two methods agree very well, although the agreement may well be accidental, considering the different assumptions and approximations made in the PIMC simulations (Born-Oppenheimer approximation, He droplets up to $N = 200$ as opposed to bulk He). Thus, using two completely different methods, we find no evidence for a metastable Mg “bubble foam” in helium. We did not consider the effects of an angular momentum barrier, since it is hard to argue how a spinning Mg dimer would not decay on a time scale of μs , and how to construct an angular momentum barrier for “bubble foam”

made of many Mg atoms. There is the possibility that metastable Mg clusters beyond dimers are stable, but at least for Mg trimers our PIMC simulations seem to rule that out.

Since spectroscopic experiments of Mg clusters in ^4He droplets were interpreted as evidence of a meta-stable “bubble foam” of Mg atoms in the helium matrix¹, a conclusive theoretical understanding of these spectra is still missing.

Acknowledgments

This work was supported, in part, by the College of Arts and Sciences, University at Buffalo SUNY, and the Austrian Science Fund Projects P21264 and I602 (to EK) and P23535 (to REZ). Discussions with Yaroslav Lutsyshyn are also acknowledged.

-
- ¹ A. Przystawik, S. Göde, T. Döppner, J. Tiggesbäumker, and K.-H. Meiwes-Broer, *Phys. Rev. A* **78**, 021202/1 (2008).
 - ² A. Hernando, M. Barranco, R. Mayol, M. Pi, and F. Ancilotto, *Phys. Rev. B* **78**, 184515 (2008).
 - ³ R. A. Aziz, F. R. W. McCourt, and C. C. K. Wong, *Molec. Phys.* **61**, 1487 (1987).
 - ⁴ J. Boronat, in *Microscopic Approaches to Quantum Liquids in Confined Geometries*, edited by E. Krotscheck and J. Navarro (World Scientific, Singapore, 2002) pp. 21–90.
 - ⁵ R. J. Hinde, *J. Phys. B (At. Mol. Opt. Phys.)* **36**, 3119 (2003).
 - ⁶ H. Partridge, J. R. Stallcop, and E. Levin, *J. Chem. Phys.* **115**, 6471 (2001).
 - ⁷ E. Tiesinga, S. Kotochigova, and P. S. Julienne, *Phys. Rev. A* **65**, 042722 (2002).
 - ⁸ M. Saarela, V. Apaja, and J. Halinen, in *Microscopic Approaches to Quantum Liquids in Confined Geometries*, edited by E. Krotscheck and J. Navarro (World Scientific, Singapore, 2002) pp. 139–205.
 - ⁹ C. E. Campbell, R. Folk, and E. Krotscheck, *J. Low Temp. Phys.* **105**, 13 (1996).
 - ¹⁰ E. Feenberg, *Theory of Quantum Fluids* (Academic, New York, 1969).
 - ¹¹ J. C. Owen, *Phys. Rev. Lett.* **47**, 586 (1981).
 - ¹² E. Krotscheck, *Phys. Rev. B* **33**, 3158 (1986).
 - ¹³ E. Krotscheck and M. Saarela, *Physics Reports* **232**, 1 (1993).

- ¹⁴ E. Krotscheck, J. Paaso, M. Saarela, K. Schörkhuber, and R. Zillich, Phys. Rev. B **58**, 12282 (1998).
- ¹⁵ A. D. Jackson, A. Lande, and R. A. Smith, Physics Reports **86**, 55 (1982).
- ¹⁶ A. D. Jackson, A. Lande, and R. A. Smith, Phys. Rev. Lett. **54**, 1469 (1985).
- ¹⁷ E. Krotscheck, R. A. Smith, and A. D. Jackson, Phys. Rev. A **33**, 3535 (1986).
- ¹⁸ A. Lande and R. A. Smith, Phys. Rev. A **45**, 913 (1992).
- ¹⁹ R. P. Feynman and A. R. Hibbs, *Quantum Mechanics and Path Integrals*, International Series in Pure and Applied Physics (McGraw-Hill, New York, 1965).
- ²⁰ D. Chandler and P. G. Wolynes, J. Chem. Phys. **74**, 4078 (1981).
- ²¹ N. Metropolis, A. W. Rosenbluth, M. N. Rosenbluth, A. H. Teller, and E. W. Teller, J. Chem. Phys. **21**, 1087 (1953).
- ²² D. M. Ceperley, Rev. Mod. Phys. **67**, 279 (1995).
- ²³ N. Blinov, X. Song, and P.-N. Roy, J. Chem. Phys. **120**, 5916 (2004).
- ²⁴ R. E. Zillich, F. Paesani, Y. Kwon, and K. B. Whaley, J. Chem. Phys. **123**, 114301 (2005).
- ²⁵ J. Boronat and J. Casulleras, Phys. Rev. B **59**, 8844 (1999).
- ²⁶ M. Mella, G. Calderoni, and F. Cargnoni, J. Chem. Phys. **123**, 054328 (2005).
- ²⁷ J. P. Toennies and A. F. Vilesov, Ang. Chem. Int. ed. **43**, 2622 (2004).
- ²⁸ A. Przystawik, S. Göde, T. Döppner, J. Tiggesbäumker, and K.-H. Meiwes-Broer, Phys. Rev. A **78**, 021202 (2008).
- ²⁹ M. Leino, A. Viel, and R. E. Zillich, J. Chem. Phys. **129**, 184308 (2008).
- ³⁰ M. Leino, A. Viel, and R. E. Zillich, J. Chem. Phys. **134**, 024316 (2011).
- ³¹ G. Auböck, J. Nagl, C. Callegari, and W. E. Ernst, Phys. Rev. Lett. **101**, 035301 (2008).
- ³² M. Saarela and E. Krotscheck, J. Low Temp. Phys. **90**, 415 (1993).